

USD 539.53

F. M. Gao, L. H. Gao (Qinhuangdao, China)

Microscopic models of hardness

Recent developments in the field of microscopic hardness models have been reviewed. In these models, the theoretical hardness is described as a function of the bond density and bond strength. The bond strength may be characterized by energy gap, reference potential, electron-holding energy or Gibbs free energy, and different expressions of bond strength may lead to different hardness models. In particular, the hardness model based on the chemical bond theory of complex crystals has been introduced in detail. The examples of the hardness calculations of typical crystals, such as spinel Si_3N_4 , stishovite SiO_2 , B_{12}O_2 , ReB_2 , OsB_2 , RuB_2 , and PtN_2 , are presented. These microscopic models of hardness would play an important role in search for new hard materials.

Key words: *hardness, bulk modulus, shear modulus, ionicity, superhard materials.*

HARDNESS TESTS

Hardness is an important mechanical property of materials. It is defined as the resistance of a material to localized deformation [1—7]. In materials science, there are two principal operational definitions of hardness: (i) Scratch hardness: Resistance to fracture or plastic deformation due to friction from a sharp object; (ii) Indentation hardness: Resistance to plastic deformation due to a constant load from a sharp indenter. Indentation hardness test is the usual type of hardness test. It can be done using Vickers as well as Knoop indenters. The Vickers test uses a symmetrical square pyramidal indenter. The Knoop test uses an asymmetrical rhombic-based pyramidal diamond indenter. In microindentation hardness testing, a pyramid is impressed into the surface of the test specimen using a known applied load of 1 to 1000 gf. The load per unit area of impression is taken as the measure of hardness:

$$H = W / S_c, \quad (1)$$

where S_c is the contact area for Vickers hardness or the projected area for Knoop hardness and W is the maximum applied load. The Knoop and Vickers hardness values differ slightly. For hard materials, their values are close enough to be within the measurement error.

Syntheses of new classes of hard and superhard materials provide new challenges for the measurement of hardness [8—15]. Since the hardness is strongly dependent on an indentation load, the load should always be reported with the hardness outcome. Brazhkin et al. [16] pointed out that necessary criteria for comparing hardness among very hard substances can be established by providing the details regarding the type of indenter, applied loads, indentation time, sample orientation, quality of the tested surface, and so on. Figure 1 shows the load dependence of the Vickers hardness for the sample of BN nanocomposite synthesized by Dubrovinskaia et al. [17]. As can be seen, its hardness even reached 145 GPa at low loads. A constant hardness is reached at loads from 4.9 to 9.8 N.

© F. M. GAO, L. H. GAO, 2010

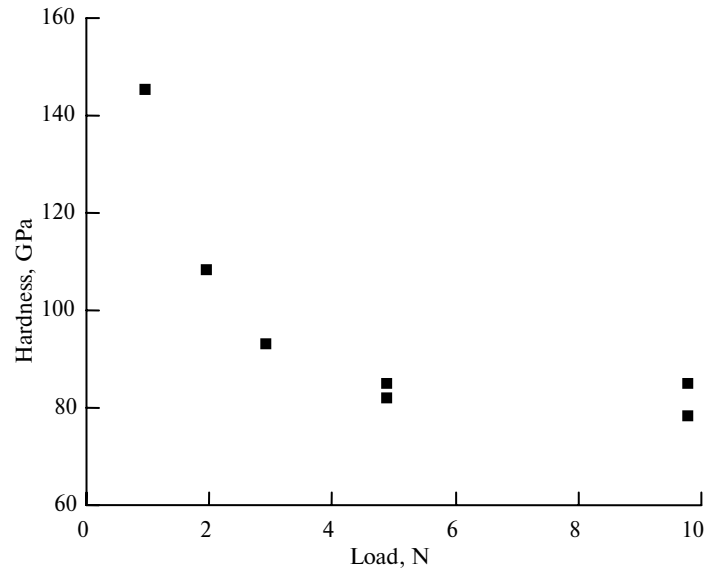


Fig. 1. Load dependence of the Vickers hardness for the sample of superhard BN nanocomposite. The loading time is 20 s. (the data from [17]).

PHYSICS OF HARDNESS

Superhard materials are defined as having a hardness of above 40 GPa. At present the experimental hardness can vary by more than 10% even for the same material; scientists have therefore been keen to devise a theoretical method for predicting the hardness of a material with a more certainty. In order to design the new superhard materials [18—30], clarifying the nature of hardness is of utmost importance. In recent years many attempts to develop a physical definition of hardness have been made.

Hardness and elastic modulus

For a material to be hard it must support the volume decrease created by the applied force, therefore, it should have a high bulk modulus. For compounds with a given bonding type, for example, the group IV elements (see Fig. 2), III—V compounds (see Fig. 3), and II—VI compounds, the hardness correlates roughly with the bulk modulus [31]. Thus, the bulk modulus was used to predict the hardness of a new material.

Ideally, one would hope to use *ab initio* computations to determine B as a function of applied strain, but this is computationally very expensive. Therefore, some empirical relations of bulk modulus were proposed [32—35]. Cohen [32] first proposed a relationship for the bulk modulus B of a compound solid, which follows:

$$B = \frac{N_c}{4} \frac{(1972 - 220f_i)}{d^{3.5}}, \quad (2)$$

where N_c is the bulk coordination number, d is the bond length, and f_i is an empirical ionicity parameter.

As pointed out in the review article by Brazhkin et al. [35], the cohesive energy (i.e. total bonding strength) is also a good correlator/predictor of bulk modulus. There is a clear correlation between the molar volume V_m , bulk modulus K and cohesive energy E_c ,

$$K \propto \frac{E_c}{V_m} \quad (3)$$

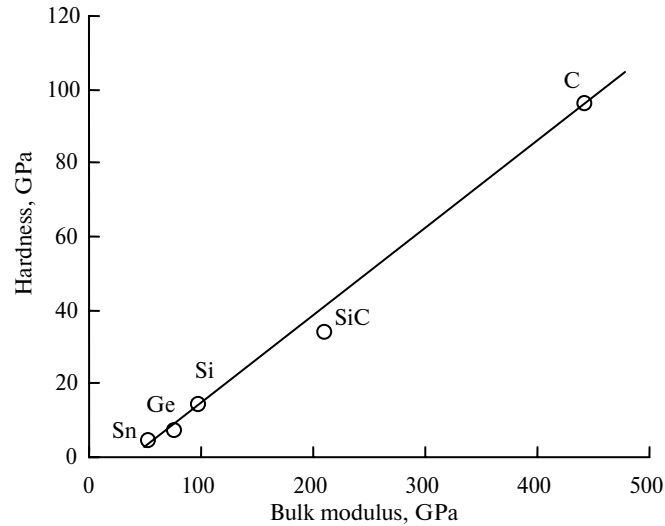


Fig. 2. Hardness vs. bulk moduli for group IV elements.

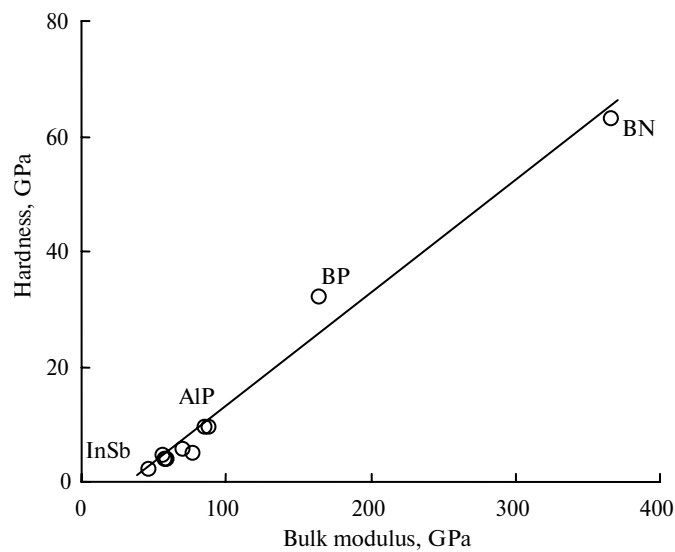


Fig. 3. Hardness vs. bulk moduli for cubic III—V compounds.

Zhang et al. [33] have studied the relation between the lattice energies and the bulk moduli of binary inorganic crystals by the concept of the lattice energy density. They have found that the lattice energy densities are in good linear relation with the bulk moduli for the same type of crystals.

Although there is a correlation between the hardness values and the bulk moduli for particular classes of materials, there are still limitations to the use of bulk modulus for predicting hardness [36]. For example, the bulk modulus of $\alpha\text{-Al}_2\text{O}_3$ exceeds that of B_{12}O_2 , however, its hardness is significantly less. The bulk modulus of Os is comparable with that of diamond, while its hardness is approximately 3.50 GPa, far smaller than that of diamond.

Teter [37] and Brazhkin et al. [35] pointed out that hardness values correlate better with shear moduli than with bulk moduli, as shown in Fig. 4. The shear modulus describes the resistance of a material to anisotropic shape change. It depends on both the plane of shear and the direction of shear. It indicates how well a material resists a tearing force. For covalent crystals, the shear modulus correlates roughly with hardness [38], which is also applicable for metals as well as ionic crystals. In order to be hard, the material must not deform in a direction different from the applied load, in other words, it must have a high shear modulus.

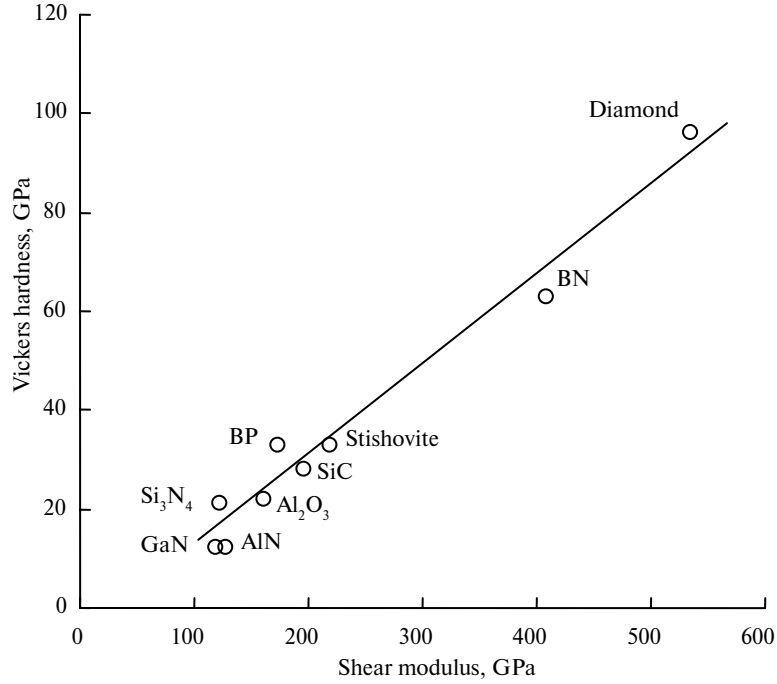


Fig. 4. Hardness vs. shear moduli.

Bulk modulus B and shear modulus G can be obtained from elastic stiffness constants C_{ij} and elastic compliance constants S_{ij} of considered crystal systems [39, 40]:

$$B_V = \frac{1}{9}(C_{11} + C_{22} + C_{33}) + \frac{2}{9}(C_{12} + C_{13} + C_{23});$$

$$B_R = \frac{1}{(S_{11} + S_{22} + S_{33}) + 2(S_{12} + S_{13} + S_{23})};$$

$$G_V = \frac{1}{15}(C_{11} + C_{22} + C_{33} - C_{12} - C_{13} - C_{23}) + \frac{1}{5}(C_{44} + C_{55} + C_{66});$$

$$G_R = \frac{15}{4(S_{11} + S_{22} + S_{33}) - 4(S_{12} + S_{13} + S_{23}) + 3(S_{44} + S_{55} + S_{66})};$$

$$B = \frac{1}{2}(B_V + B_R);$$

$$G = \frac{1}{2}(G_V + G_R).$$

Theoretical definition of hardness

Although the better correlation has been observed between the hardness and *shear modulus*, the dependence is not yet unequivocal and monotonic [35]. For example, the bulk and shear moduli of tungsten carbide are as high as 439 and 282 GPa, respectively, which are among the highest as known, but its hardness is only 30 GPa [27]. Indeed, there is no one-to-one correspondence between hardness and bulk modulus or shear modulus.

For theoretical study, an appropriate definition of hardness is necessary and essential. Gao et al. [41, 42] took an important step towards the goal of theoretical characterization of hardness by developing a semi-empirical formula for the hardness of a material based on ionicity, bond length, and the number of electrons available for bonding, and succeeded in estimating the hardness of a number of covalent materials using the semi-empirical formulae.

Gao et al. [41] pointed out that the hardness of covalent crystals is intrinsic and equivalent to the sum of resistance of each bond per unit area to the indenter. In an indentation test, the bond breaking can occur. According to Gilman's assumption [38], energetically breaking an electron-pair bond inside a crystal means that two electrons become excited from the valence band to the conduction band. In other words, the resistant force of bond can be characterized by energy gap E_g . Based on this assumption, the hardness of covalent crystals should have the form:

$$H \text{ (GPa)} = AN_a E_g, \quad (4)$$

where A is the proportional coefficient and N_a is the covalent bond number per unit area.

Following Gao's work, Šimůnek and Vackar [43, 44] proposed another expression for hardness by introducing the bond strength concept

$$H = \frac{C}{\Omega} S_{ij}, \quad (5)$$

where C is the proportional coefficient and Ω is the volume of a pair of ij atoms. S_{ij} is the bond strength between atoms i, j .

Recently, Li et al. [45, 46] have also suggested a hardness formula:

$$H = pN_V X_{ab} + q, \quad (6)$$

where p and q are the constants, N_V is the bond density, X_{ab} is the bond electronegativity and,

$$X_{ab} = \sqrt{\frac{X_a}{N_a} \frac{X_b}{N_b}}, \quad (7)$$

where X_a and X_b are the electronegativity of atoms a and b , respectively. N_a and N_b are the coordination numbers of atoms a and b , respectively.

More recently, based on Gibbs free energy of atomization ΔG_{at}^{θ} , Mukhanov et al. [47] have proposed a thermodynamic formula for the hardness calculations:

$$H = \frac{2\Delta G_{at}^{\theta}}{VN} \alpha \beta \epsilon, \quad (8)$$

where V is the molar volume, N is the maximum coordination number, α is the coefficient of the relative plasticity, β is the coefficient allowing for a contribution of the bond polarity, ϵ is the ratio of the amount of valent electrons per atom to the amount of bonds that this atom forms with the neighboring atoms.

In addition, the work of Gilman [38] indicates that the hardness can often be related to a shear instability such as associated with a structural phase transition in tetrahedral semiconductors.

CALCULATIONS OF CHEMICAL BOND IONICITY AND HARDNESS

Chemical bond ionicity

As mentioned above, the ionicity of chemical bond plays a significant role in mechanical properties such as hardness, bulk modulus. According to Pauling's rule [48], if we consider a crystal, in which cation A, carrying a charge $+Ze$, is coordinated by N anions B, then each A—B bond is said to have a Pauling bond valence of $Q_{AB} = Z/N$. In a stable coordinated structure the total bond valence of the bonds that reach an anion from all the neighboring cations is equal to the charge of the anion. Then, the ionicity of A—B bond can be calculated as follows:

$$f_i = 1 - Q_{AB} \exp \frac{-(X_A - X_B)^2}{4}, \quad (9)$$

where X_A and X_B are the electronegativity of atoms A and B, respectively.

Another noted scale of ionicity is Phillips' ionicity. Phillips' criterion for the ionicity is more accurate spectroscopically than that of Pauling, which is based on the data on heats of the formation of solids [49, 50].

Reviews concerning the bond ionicity and its application had been made by Phillips [51], Van Vechten [52, 53], Levine [54, 55]. However, it is known that PVL (Phillips-Van Vechten-Levine) theory can deal with binary crystals only. In order to calculate the bond ionicity of a multicomponent crystal, the multicomponent crystal must be decomposed into pseudobinary crystals containing only one type of chemical bond. A crucial method decomposing the complex crystal into pseudobinary crystals each containing only one type of chemical bond is proposed by Zhang [56, 57]. For the multibond crystal $A_aB_b\dots$, the subformula for any kind of chemical bond A—B can be expressed as:

$$\left[\frac{N(B-A)a}{N_{CA}} \right]_A \left[\frac{N(A-B)b}{N_{CB}} \right]_B, \quad (10)$$

where A, B, ... represent different elements or different sites of the same element in the crystal formula, and a, b, \dots represent numbers of the corresponding element, $N(B-A)$ represents the number of B ions in the coordination group of the A ion, and N_{CA} represents the nearest coordination number of the A ion. These binary crystals are related to each other, and every binary crystal includes only one type of chemical bond. However, the properties of these pseudobinary crystals are different from those of real binary crystals, although their chemical bond parameters can be calculated in a similar way.

Equation (10) also can be rewritten in another form

$$\frac{N(B-A)a}{N_{CA}} AB_n \quad (11)$$

and

$$n = \frac{N(A-B)bN_{CA}}{N(B-A)aN_{CB}}, \quad (12)$$

where the prefix $N(B-A)a/N_{CA}$ represents the relation between the number of B ions and the total number of ions bonded to the central A ion, and the subscript $[N(A-B)bN_{CA}]/[N(B-A)aN_{CB}]$ represents the ratio of the element B to A, n . According to Eq. (11), each type of bond has its corresponding subformula, and the sum of all subformulae equals the crystal formula, which is called the bond-valence equation.

After decomposing a complex crystal into different kinds of pseudobinary crystals, which form an isotropic system, and introducing an effective charge of a valence electron by Pauling's bond valence method [48], PVL theory can be used directly to calculate the chemical bond parameters in a complex crystal compound.

By analogy with the work of PVL, average energy gap E_g^μ for every μ bond in pseudobinary crystals can be separated into homopolar E_h^μ and heteropolar C^μ parts.

Homopolar gap E_h^μ can be interpreted as produced by the symmetric part of the total potential, while the ionic or charge-transfer gap C^μ results from the effect of the antisymmetric part. The average valence-conduction band gap is given by

$$(E_g^\mu)^2 = (E_h^\mu)^2 + (C^\mu)^2. \quad (13)$$

The ionicity and covalency of any type of chemical bond is defined as follows:

$$f_i^\mu = (C^\mu)^2 / (E_g^\mu)^2; \quad (14)$$

$$f_c^\mu = (E_h^\mu)^2 / (E_g^\mu)^2 \quad (15)$$

and

$$E_h^\mu = 39.74 / (d^\mu)^{2.48} \text{ (eV)}, \quad (16)$$

where d^μ is the bond length. For any binary crystal, i.e. AB_n type compounds, heteropolar C^μ part is defined as

$$C^\mu = 14.4b^\mu \left[(Z_A^\mu)^* + \Delta Z_A^\mu - n(Z_B^\mu)^* \right] \frac{e^{-k_s^\mu r_0^\mu}}{r_0^\mu} \text{ (eV)}; \quad (17)$$

$$r_0^\mu = \frac{d^\mu}{2};$$

$$k_s^\mu = \left(\frac{4k_F^\mu}{\pi a_B} \right)^{1/2} = 1.551(k_F^\mu)^{1/2}; \quad (18)$$

$$(k_F^\mu)^3 = 3\pi^2 N_e^\mu; \quad (19)$$

$$N_e^\mu = \frac{(n_e^\mu)^*}{v_b^\mu}; \quad (20)$$

$$(n_e^\mu)^* = \frac{(Z_A^\mu)^*}{N_{CA}^\mu} + \frac{(Z_B^\mu)^*}{N_{CB}^\mu}; \quad (21)$$

$$v_b^\mu = \frac{(d^\mu)^3}{\sum_v [(d^v)^3 N_b^v]}, \quad (22)$$

where v_b^μ is the bond volume, $(n_e^\mu)^*$ is the number of effective valence electrons per μ bond, N_e^μ is the number of valence electrons of μ bond per cubic centimeter. k_F^μ and k_s^μ are Fermi wave number and Thomas-Fermi screening wave number of valence electrons in a binary crystal composed of only one type of bond μ , respectively. a_B is the Bohr radius and n is the ratio of element B to element A in the subformula. $(Z_A^\mu)^*$ and $(Z_B^\mu)^*$ are the numbers of effective valence electrons of the A and B ions, respectively, and $(Z_A^\mu)^* = Q_{AB}^\mu N_{CA}^\mu$, $(Z_A^\mu)^* = [(Q_{AB}^\mu N_{CB}^\mu)/(8 - Z_B^\mu)] Z_B^\mu$, Q_{AB}^μ is the Pauling bond valence of A—B bonds, Z_B^μ is the number of valence electrons of the B atoms. ΔZ_A^μ is the correction factors from d electron effects such as the crystal field stable energy and Janh-Teller effect, etc. [58, 59], b^μ is proportional to the square of the average coordination number N_c^μ

$$b^\mu = \beta(N_c^\mu)^2; \quad (23)$$

$$N_c^\mu = \frac{N_{CA}^\mu}{1+n} + \frac{nN_{CB}^\mu}{1+n}, \quad (24)$$

where b^μ depends on a given crystal structure. The typical value of β is $0.089 \pm 10\%$ [54].

If the dielectric constant of the crystal is known, the value of β can be deduced from the Kramers-Kronig relation of dielectric function at the long wave limit, which is written as

$$\chi^\mu = \frac{4\pi N_e^\mu e^2 D^\mu}{m(E_g^\mu)^2} \cdot \left(1 - \frac{E_g^\mu}{4E_F^\mu} + \frac{(E_g^\mu)^2}{48(E_F^\mu)^2} \right); \quad (25)$$

$$\varepsilon(\infty) = 1 + \chi = 1 + \sum_\mu F^\mu \chi^\mu, \quad (26)$$

where χ is the macroscopic linear susceptibility, χ^μ is the total macroscopic susceptibility of a binary crystal composed of only one type of bond μ , E_F^μ is the Fermi energy, F^μ is the fraction of the binary crystal composing the actual complex crystal. D^μ is the periodic dependent constants tabulated in [54].

Hardness of polar covalent crystal

Equation (4) is suitable for the hardness calculations of pure covalent crystals only. For polar covalent crystals, besides covalent component, partial ionic bonding has to be considered. Ionic bonding results from long-range electrostatic force, which is not directly related to hardness [38]. Phillips' homopolar band gap E_h characterizes the activation energies of dislocation glide in polar covalent crystals and the strength of the covalent bonding. On the other hand, the partial ionic bonding results in the loss of covalent bond charge, further results in a smaller effective covalent bond number per unit area (N_a) in comparison with that of pure covalent crystals. This screening effect can be described by a correction factor, $e^{-1.191f_i}$. The hardness of polar covalent crystals is expressed as follows [41]:

$$H_V(\text{GPa}) = 14(N_a e^{-1.191f_i}) E_h; \quad (27)$$

$$N_a = \left(\sum \frac{n_i Z_i}{2V} n_i Z_i / 2V \right)^{2/3}, \quad (28)$$

where n_i is the number of the i th atom in the cell, Z_i is the valence electron number of the i th atom. Also Eq. (27) can be expressed as:

$$H_V(\text{GPa}) = 556 \frac{N_a e^{-1.191f_i}}{d^{2.5}} = 350 \frac{N_e^{2/3} e^{-1.191f_i}}{d^{2.5}}, \quad (29)$$

where d is the bond length.

The Vickers hardness of diamond measured under 9.8 N loads is about 96 GPa, which is in agreement with the calculated hardness [41]. The calculated hardness of $\alpha\text{-Al}_2\text{O}_3$, 21 GPa, is in agreement with its Vickers hardness measured under 2.5 N loads [60]. The calculated hardness of stishovite (SiO_2) is 30 GPa [41]. An appreciable scatter in hardness measurements of stishovite was observed, ranging from 21 to 33 GPa [61]. The hardness of a stishovite single crystal determined from the Vickers diamond pyramid hardness tests under 2 N loads is 31.8 ± 1.0 GPa along the c -axis and 26.2 ± 1.0 GPa along a perpendicular direction [62]. Therefore, a comparison of values from different studies is only of a limited significance. Here we suggest that calculated hardness values may correspond to a comparative Vickers hardness tested under a comparative load that is taken approximately as $\frac{9.8\text{N}}{H_V^{dia}} H_V^{cal}$, where H_V^{dia} is the Vickers hardness of diamond under 9.8 N loads

and H_V^{cal} is the calculated hardness.

Hardness of multicomponent compound systems

The hardness surely involves the cooperative softening of many bonds. When there are differences in the strength among different types of bonds, the trend of breaking the bonds will start from a softer one. The hardness of multicomponent compound systems can be expressed as a geometric average of hardness of all pseudobinary systems in the solid [41],

$$H_V = \left[\prod (H_V^{\mu})^{n^{\mu}} \right]^{1/\sum n^{\mu}}, \quad (30)$$

where n^μ is the number of bonds of type μ composing the actual complex crystal. The hardness, H_V^μ , of pseudobinary compound composed of μ -type bond can be calculated using Eqs. (27)—(29).

Nevertheless, it should be noted that Eq. (30) has to be applied with care in systems with large anisotropy, in which n^μ will vary along the different directions of the crystal.

γ - Si_3N_4 . Recently, it has been reported that cubic Si_3N_4 (γ - Si_3N_4) with a cubic spinel structure could be synthesized at pressures above 15 GPa and temperatures exceeding 2,000 K, yet persists metastably in air at an ambient pressure to at least 700 K [63]. This new superhard cubic Si_3N_4 phase opens considerable industrial scope in materials science [64, 65].

Equilibrium structural parameters for the γ - Si_3N_4 spinels calculated by using the GGA are $a = 7.65 \text{ \AA}$, $u = 0.382$ [66]. In this structure the Si atom is in octahedral coordination with six N atoms (denoted as Si^o) and simultaneously in tetrahedral coordination with four N atoms (denoted as Si^t).

Pauling [48] pointed out that crystal structures obey the Electrostatic Valency Principle: an ionic structure will be stable to the extent that the sum of the Pauling bond valence, Q_{AB}^μ , of the bonds that reach an ion equal to the charge on that ion. For example, in Fig. 5 each Si^{4+} is surrounded by 4N^{3-} ions. The Si^t is thus in 4 fold coordination. Thus, $Q_{AB}^\mu = 1$. That's to say each N ion contributes one negative charge to the Si^t . So the +4 charge on the Si^t ion is balanced by $4 \times 1 = 4$ negative charge from the 4N ions.

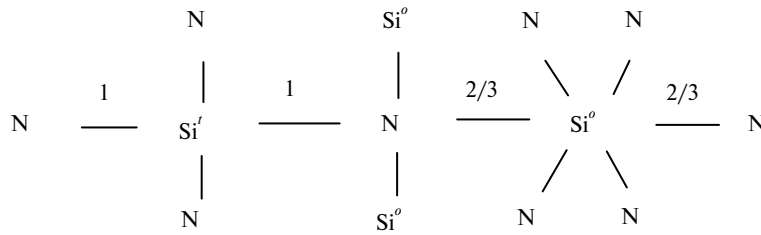


Fig. 5. Coordination and Pauling bond valence in γ - Si_3N_4 .

According to Eq. (13), γ - Si_3N_4 can be decomposed into the sum of pseudobinary crystals as follows:

$$\begin{aligned} \gamma\text{-Si}_3\text{N}_4 &= \text{Si}^t\text{Si}^o_2\text{N}_4 = \\ &= \left[\frac{N(N - \text{Si}^t)a}{N_C \text{Si}^t} \right] \text{Si}^t \left[\frac{N(\text{Si}^t - N)b}{N_C N} \right] \text{N} + \left[\frac{N(N - \text{Si}^o)a}{N_C \text{Si}^o} \right] \text{Si}^o \left[\frac{N(\text{Si}^o - N)b}{N_C N} \right] \text{N} = \\ &= \frac{4 \times 1}{4} \text{Si}^t \frac{1 \times 4}{4} \text{N} + \frac{6 \times 2}{6} \text{Si}^o \frac{3 \times 4}{4} \text{N} = \text{Si}^t\text{N} + 2\text{Si}^o\text{N}_{3/2}. \end{aligned}$$

From Fig. 5 it is seen that the Pauling bond valence, Q_{AB}^μ , of the Si^t —N and Si^o —N bonds are 1 and 2/3, respectively. For Si^tN , $(Z_A^\mu)^* = Q_{AB}^\mu N_{CA}^\mu = 1 \times 4 = 4$, $(Z_B^\mu)^* = [(Q_{AB}^\mu N_{CB}^\mu)/(8 - Z_B^\mu)] Z_B^\mu = [(1 \times 4)/(8 - 5)] \times 5 = 20/3$. For $\text{Si}^o\text{N}_{3/2}$,

$$(Z_A^\mu)^* = Q_{AB}^\mu N_{CA}^\mu = (2/3) \times 6 = 4, \quad (Z_B^\mu)^* = [(Q_{AB}^\mu N_{CB}^\mu)/(8 - Z_B^\mu)] Z_B^\mu = [(2/3) \times 4]/(8-5) \times 5 = 40/9.$$

The bond volumes of the Si^t—N and Si^o—N bonds, v_b^μ (Si^tN) and v_b^μ (Si^oN), may be calculated as follows:

$$v_b^\mu(\text{Si}^t\text{N}) = [d(\text{Si}^t\text{N})]^3 / \left\{ \frac{[d(\text{Si}^t\text{N})]^3 N(\text{Si}^t) n(\text{Si}^t) + [d(\text{Si}^o\text{N})]^3 N(\text{Si}^o) n(\text{Si}^o)}{V} \right\} =$$

$$= 1.75^3 / \left(\frac{1.75^3 \times 4 \times 8 + 1.86^3 \times 6 \times 16}{7.65^3} \right) = 3.04,$$

$$v_b^\mu(\text{Si}^o\text{N}) = [d(\text{Si}^o\text{N})]^3 / \left\{ \frac{[d(\text{Si}^t\text{N})]^3 N(\text{Si}^t) n(\text{Si}^t) + [d(\text{Si}^o\text{N})]^3 N(\text{Si}^o) n(\text{Si}^o)}{V} \right\} =$$

$$= 1.86^3 / \left(\frac{1.75^3 \times 4 \times 8 + 1.86^3 \times 6 \times 16}{7.65^3} \right) = 3.65$$

where V is the cell volume, $d(\text{Si}^t\text{N})$ and $d(\text{Si}^o\text{N})$ are the lengths of the Si^t—N and Si^o—N bonds, respectively. $N(\text{Si}^t)$ and $N(\text{Si}^o)$ are the coordination numbers of the Si^t and Si^o atoms, respectively. $n(\text{Si}^t)$ and $n(\text{Si}^o)$ are the numbers of the Si^t and Si^o atoms in a cell, respectively.

As shown in Table 1, the calculated hardness values of the Si^t—N and Si^o—N bonds are 57.9 GPa and 25.1 GPa, respectively. The average hardness of the γ -Si₃N₄ spinels can be calculated as follows:

$$H_V = \left[\prod_{\mu} (H_V^\mu)^{n^\mu} \right]^{1/\sum n^\mu} =$$

$$\left\{ [H_V^\mu(\text{Si}^t\text{N})]^{N(\text{Si}^t) \cdot n(\text{Si}^t)} [H_V^\mu(\text{Si}^o\text{N})]^{N(\text{Si}^o) \cdot n(\text{Si}^o)} \right\}^{1/[N(\text{Si}^t) \cdot n(\text{Si}^t) + N(\text{Si}^o) \cdot n(\text{Si}^o)]} =$$

$$= (57.9^{4 \times 8} \times 25.1^{6 \times 16})^{1/(4 \times 8 + 6 \times 16)} = 30.9 \text{ (GPa)}.$$

Table 1. Chemical bond parameters and hardness of cubic γ -Si₃N₄ spinels, which are estimated by using $\beta = 0.089$. Structural parameters are from the results obtained within the GGA, where $H_{V\text{av}}$ (average hardness) is calculated

γ -Si ₃ N ₄ (GGA)	Bond type	Q_{AB}^μ	N_C^μ	$(Z_A^\mu)^*$	$(Z_B^\mu)^*$	$(n_e^\mu)^*$	d^μ , Å	v_b^μ , Å ³	N_e^μ , Å ⁻³	E_h^μ , eV	C^μ , eV	f_i^μ	H_V^μ	$H_{V\text{av}}$, GPa
$a = 7.65$ Å	Si ^t N	1	4	4	20/3	8/3	1.75	3.04	0.87	9.91	6.04	0.27	57.9	30.9
[66]														
$u = 0.382$	Si ^o N _{3/2}	2/3	4.8	3	40/9	16/9	1.86	3.65	0.49	8.55	8.94	0.52	25.1	

The measured hardness values of γ -Si₃N₄ are still quite controversial. From the correlation between the Vickers hardness and shear modulus presented by Teter [37], Soignard et al. estimated the hardness of γ -Si₃N₄ at a value of 30 GPa [67]. Jiang et al. [68] reported a Vickers hardness of 32.78—37.27 GPa for a

polycrystalline sample. But the applied loading conditions were not clearly described. Based on the nanoindentation tests under 5 mN loads, the Vickers microhardness of dense γ - Si_3N_4 was estimated to be between 30 and 43 GPa [69]. Here, our calculated hardness of γ - Si_3N_4 spinels, 30.9GPa, should be corresponding to the Vickers hardness under about 3N loads.

ReB₂, OsB₂ and PtN₂. ReB_2 [70, 71], OsB_2 [72] and PtN_2 [73] have attracted considerable attention due to their superior mechanical properties. PtN_2 with the pyrite structure is a semiconductor. ReB_2 with the hexagonal structure and OsB_2 with the orthorhombic structure possess stronger covalency and weaker metallicity like WC. In [41] the calculated hardness of WC is in agreement with its experimental value. This implies that the method mentioned above may be employed to estimate the hardness of ReB_2 and OsB_2 .

According to Eq. (13), ReB_2 , OsB_2 , and PtN_2 can be decomposed into the sum of pseudobinary crystals as follows:

$$\text{ReB}_2 = 3/4\text{ReB}_{8/7} + 1/4\text{ReB}_{8/7} + 3/7\text{BB};$$

$$\text{OsB}_2 = 1/2\text{OsB}_{8/7} + 1/4\text{OsB}_{8/7} + 1/4\text{OsB}_{8/7} + 2/7\text{BB} + 1/7\text{BB};$$

$$\text{PtN}_2 = \text{PtN}_{3/2} + 1/4\text{NN}.$$

From Fig. 6 it is seen that Pauling bond valence values Q_{AB}^μ of the Re—B and B—B bonds are 1/2 and 1/3, respectively. The ionicity of pseudobinary compound composed of the μ -type bond in these compounds can be calculated using Eqs. (13)—(22). The N_a of pseudobinary compound $\text{ReB}_{8/7}$ may be obtained using Eq. (28) as,

$$N_a = \left(\frac{Q_{\text{AB}}^\mu N_{\text{CA}}^\mu + \frac{8}{7} Q_{\text{AB}}^\mu N_{\text{CB}}^\mu}{2N_{\text{CA}}^\mu v_b^\mu} \right)^{2/3} = \left(\frac{\frac{1}{2} \times 8 + \frac{8}{7} \times \frac{1}{2} \times 7}{2 \times 8 \times v_b^\mu} \right)^{2/3},$$

where the valence electron of B is 3. The N_a of pseudobinary compound $\text{PtN}_{3/2}$ may be calculated using Eq. (28) as,

$$N_a = \left[\left(Q_{\text{AB}}^\mu N_{\text{CA}}^\mu + \frac{3}{2} Q_{\text{AB}}^\mu N_{\text{CB}}^\mu \frac{Z_{\text{B}}^\mu}{8 - Z_{\text{B}}^\mu} \right) / (2N_{\text{CA}}^\mu v_b^\mu) \right]^{2/3} = \\ = \left[\left(\frac{1}{3} \times 6 + \frac{3}{2} \times \frac{1}{3} \times 4 \times \frac{5}{3} \right) / (2 \times 6 \times v_b^\mu) \right]^{2/3}$$

where the valence electron of N atom, Z_{B}^μ , is 5. The calculated results are listed in Table 2.

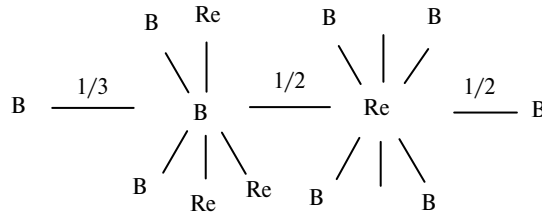


Fig. 6. Coordination and Pauling bond valence in ReB_2 .

Table 2. Chemical bond parameters and hardness of ReB₂, OsB₂, RuB₂ and PtN₂, which are estimated by using $\beta = 0.089$. Where $H_{V_{av}}$ and $H_{V_{exp}}$ are the calculated and experimental Vickers hardness, respectively E_h^μ

	Bond type	Q_{AB}^μ	N_c^μ	$(Z_A^\mu)^*$	$(Z_B^\mu)^*$	$(n_e^\mu)^*$	$d^\mu, \text{\AA}$	$v_b^\mu, \text{\AA}^3$	$N_e^\mu, \text{\AA}^{-3}$	Z_A^μ	E_h^μ, eV	C^μ, eV	f_i^μ	$N_a^\mu, \text{\AA}^{-2}$	H_V^μ	$H_{V_{av}}, \text{GPa}$	$H_{V_{exp}}, \text{GPa}$
ReB ₂	ReB _{8/7}	1/2	7.47	4	35/6	4/3	2.257	2.874	0.464	2.090	5.278	2.435	0.175	0.312	18.4	23.7	26.9
	ReB _{8/7}	1/2	7.47	4	35/6	4/3	2.226	2.757	0.483	2.045	5.462	2.703	0.196	0.320	19.1		[74]
	BB	1/3	7	7/3	7/3	2/3	1.82	1.507	0.442		9.000	0	0	0.366	45.5		(294N)
OsB ₂	OsB _{8/7}	1/2	7.47	4	35/6	4/3	2.215	2.787	0.478	1.978	5.530	3.073	0.236	0.318	18.3		
	OsB _{8/7}	1/2	7.47	4	35/6	4/3	2.148	2.542	0.525	1.888	5.967	3.734	0.281	0.338	19.9		
	OsB _{8/7}	1/2	7.47	4	35/6	4/3	2.308	3.154	0.423	2.104	4.993	2.281	0.173	0.293	16.4		
	BB	1/3	7	7/3	7/3	2/3	1.875	1.691	0.394		8.360	0	0	0.339	39.1		
	BB	1/3	7	7/3	7/3	2/3	1.8	1.496	0.446		9.250	0	0	0.368	47.0		
RuB ₂	RuB _{8/7}	1/2	7.47	4	35/6	4/3	2.199	2.727	0.489	1.956	5.630	3.223	0.247	0.323	18.6		
	RuB _{8/7}	1/2	7.47	4	35/6	4/3	2.165	2.603	0.512	1.911	5.852	3.558	0.270	0.333	19.5		
	RuB _{8/7}	1/2	7.47	4	35/6	4/3	2.252	2.929	0.455	2.028	5.307	2.741	0.211	0.308	17.5		
	BB	1/3	7	7/3	7/3	2/3	1.902	1.765	0.378		8.068	0	0	0.329	36.7		
	BB	1/3	7	7/3	7/3	2/3	1.774	1.432	0.466		9.590	0	0	0.378	50.2		
PtN ₂	PtN _{3/2}	1/3	4.8	2	20/9	8/9	2.087	4.454	0.200	1.697	6.409	1.169	0.032	0.215	18.3		
	NN	2	4	8	8	4	1.405	1.359	0.943		17.100			1.294	307.2		

The calculated average hardness of ReB₂ is 23.7 GPa, which is close to the measured comparative Vickers hardness of ReB₂ under 2.94 N loads, 26.9±1.3 GPa [74]. According to the bond lengths existing in the cell, all B—B and Os—B bonds per unit cell of the OsB₂ with the orthorhombic structure could be classified into five groups, with lengths of 1.875, 1.800, 2.215, 2.148, and 2.308 Å, respectively. As shown by the dotted line in Fig. 7, there are only Os—B bonds with a bond length of 2.308 Å in the (100)[010] direction. These bonds are the softest. Therefore, the (001) plane of OsB₂ could be the easiest *slip planes*. According to [41], the weakest bond plays a determinative role in the hardness of materials. *We may expect that the hardness of OsB₂ would be smaller in the direction parallel to the easy-slip planes, i.e., the (001) planes.* The calculated average hardness of OsB₂ is 22.8 GPa. The calculated hardness of the pseudobinary compound composed of Os—B bonds of bond length 2.308 Å, 16.4 GPa, is much closer to the measured comparative Vickers hardness of OsB₂ under the 1.96 N load, 17.8 ± 0.7 GPa [74]. Similarly, the calculated hardness of the pseudobinary compound composed of Ru—B bonds of bond length 2.252 Å, 17.5 GPa is close to

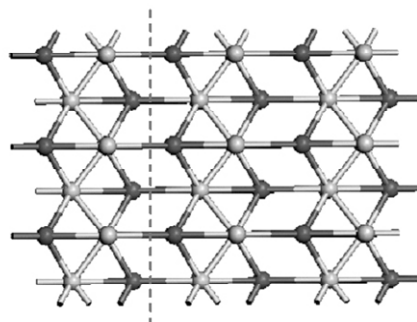


Fig. 7. Bonding structure of the (100) plane of OsB₂. The vertical dotted line indicates the (100)[010] direction.

the measured comparative Vickers hardness of RuB₂ under 1.96 N load, 15.1 ± 1.1 GPa [74].

The calculated hardness of the pseudobinary compound PtN_{3/2} in PtN₂ is 18.6 GPa. The hardness of N—N bonds is 307 GPa, which is far greater than that of a diamond indenter. Thus, the N—N bonds might not break in a hardness test. Similarly, for the compounds with anionic cluster, for example CaCO₃, its C—O bond may not break in a hardness test. The anionic cluster CO₃ would slip as one unit under the indenter, and does not contribute to the hardness of CaCO₃. The hardness of CaCO₃ results just from the resistance of the Ca—O bond.

Hardness of boron icosahedral structured materials

The structure of α -rhombohedral boron contains a huge hole along the *c*-axis between the icosahedra. In Fig. 8 the dotted lines show the 3-centre bonds between the 6 equatorial boron atoms in each icosahedron and 6 other icosahedra in the same sheet at 2.025 Å. The sheets are stacked so that each icosahedron is bonded by six 2-centre B—B bonds. B₁₂ units in the layer above are centered over 1 and those in the layer below are centered under 2 [75]. In the boron carbide structure the huge hole accommodates a three-atom chain. In the structures of B₁₂O₂ the O atoms form pairs instead of three-atom chains [76].

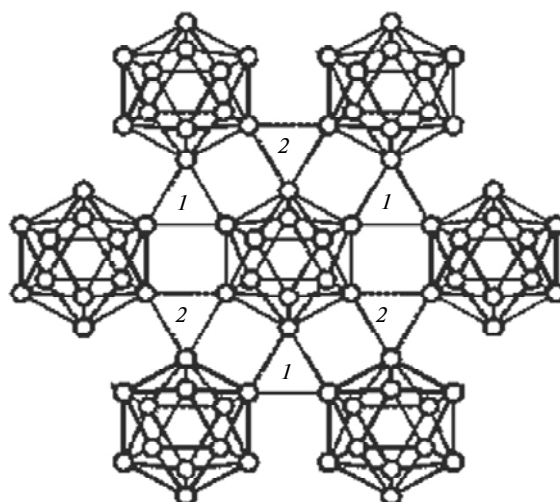


Fig. 8. Basal plane of α -rhombohedral boron. The dotted triangles denoted as 1 or 2 show the 3-centre bonds between the 6 equatorial boron atoms in each icosahedron to 6 other icosahedra.

The α -rhombohedral form of boron is the simplest one in boron-rich solids. The 36 valence electrons of each B₁₂ unit are distributed as follows: 26 electrons just form the 10 3-centre/2-electron bonds (denoted BBB1) and 3 normal 2-centre/2-electron bonds (denoted BB1) within the icosahedron and 6 electrons share with 6 other electrons from 6 neighboring icosahedra in adjacent planes to form the rhombohedrally directed normal 2-centre/2-electron bonds (denoted BB2); this leaves 4 electrons, which is just the number required for contribution to the 6 equatorial 3-centre/2-electron bonds (denoted BBB2). Thus, α -boron has 4 bond types. B₁₂ can be decomposed into the sum of pseudobinary crystals as follows [77, 78]:

$$B_{12} = 10 (BBB1) + 3 (BB1) + 2 (BBB2) + 3 (BB2), \quad (31)$$

where the coefficient is the number of bonds in cell.

$B_{12}O_2$ has the same space group $R\bar{3}m$ as B_{12} [79]. Each of the two oxygen atoms links to three B_{12} icosahedral, while oxide atoms are not bonding, see Fig. 9. It can be decomposed into the sum of pseudobinary crystals as follows:

$$B_{12}O_2 = 10 (BBB1) + 3 (BB1) + 3 (BB2) + 6 (BO_{4/3}). \quad (32)$$

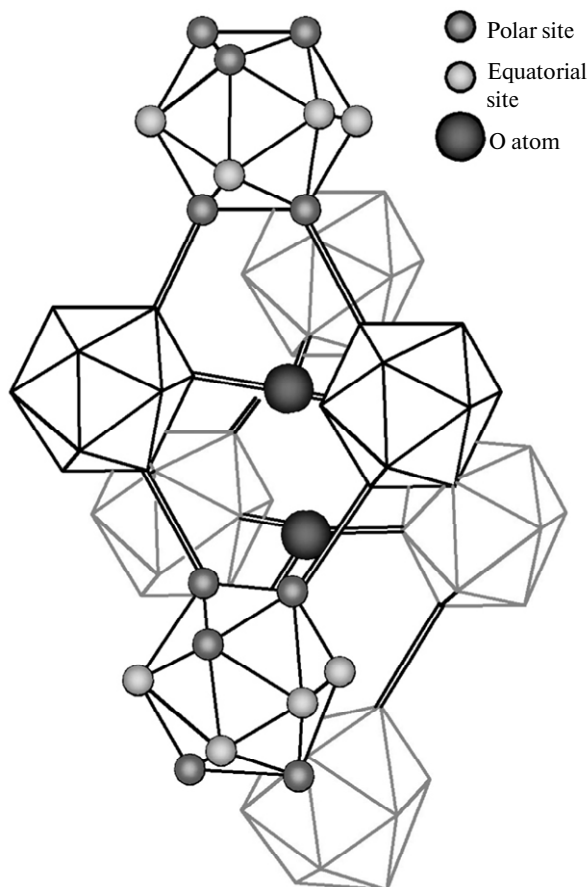


Fig. 9. Atomic structure of $B_{12}O_2$.

The distinct feature of the chemical bonding of boron solids is three-center or icosahedral bonding. Thus, the first problem of extending Eq. (29) to boron-rich systems is how the bond length of three-center bonds is determined. For 2-centre/2-electron bonds, the bond length is defined by the distance between two nuclei of bonding atoms. In Fig. 10 we employ sp^x hybrid orbitals to show the sketch of the 2-centre/2-electron bond and 3-centre/2-electron bond. For 3-centre/2-electron bonds, the bond length can be taken as the diameter of a circle shown in Fig. 10. If the distances (denoted l) between pairs of atoms in the 3-centre/2-electron bond are equal, the bond length of 3-centre/2-electron bonds d_{3c2e} can be expressed as [77]:

$$d_{3c2e} = \frac{2}{\sqrt{3}} l. \quad (33)$$

The calculated results of hardness and chemical bond parameters of $B_{12}O_2$ are shown in Table 3.

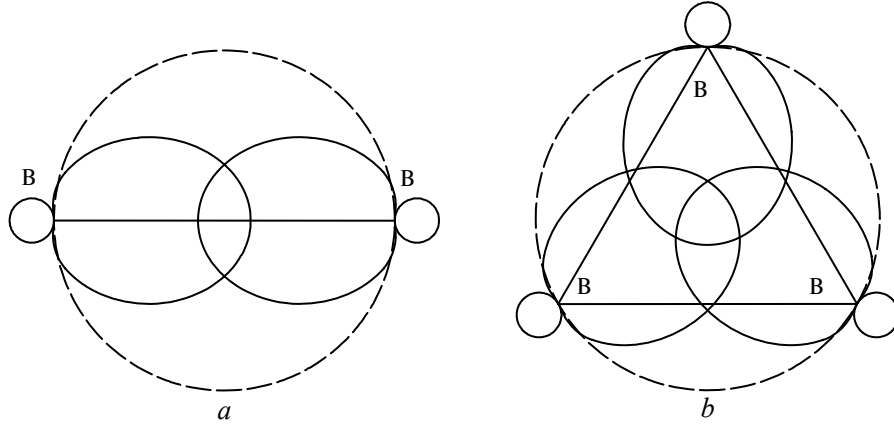


Fig. 10. Sketch of the 2-centre/2-electron bond (a) and 3-centre/2-electron bond (b).

Table 3. Hardness and chemical bond parameters of $B_{12}O_2$, where H_{Vav} are calculated

Bond type	d^μ , Å	v_b^μ , Å ³	N_e^μ , Å ⁻³	E_h^μ , eV	f_i^μ	H_V^μ	H_{Vav} , GPa
BB1	1.798	4.270	0.468	9.276	0.000	49.3	44.6
BBB1	2.076	6.573	0.304	6.494	0.000	25.9	
BB2	1.664	3.385	0.591	11.240	0.000	69.8	
BO _{4/3}	1.476	2.362	1.073	15.132	0.460	83.7	

Recently the orthorhombic B_{28} single crystal [9, 10] and $B_{13}N_2$ have been synthesized [80]. The measured Vickers hardness of the orthorhombic B_{28} is about 39–61 GPa under 4.9 N loads [81]. The calculated hardness of the orthorhombic B_{28} and $B_{13}N_2$ by Mukhanov et al. is 48.8 GPa and 40.3 GPa, respectively [47]. The calculated hardness of $B_{13}N_2$ by Gou et al. is 40.8 GPa [82]. These indicate that they are two new superhard materials.

Hardness of nanocrystals

In nanocrystals, the conduction/valence band edges shift generally to higher energy relative to the bulk material when the crystal size is decreased [83]. According to the Kubo theory [84], the band gap ($E_{g\ nano}$) of a nanocrystal should increase inversely with the volume V , the energy shift δ is given by

$$\delta = \frac{2\hbar^2\pi^2}{mV(3\pi^2N_e)^{1/3}} = \frac{b}{DN_e^{1/3}}, \quad (34)$$

where b is the constant, D is the cluster diameter and N_e is the electron density of the material, and

$$E_{g\ nano} = E_{g\ bulk} + \delta, \quad (35)$$

where $E_{g\ bulk}$ is the band gap energy of the bulk material.

An expression for the hardness including quantum confinement effects for nanocrystals can be obtained by substituting Eq. (34) into Eq. (4) [85],

$$H \text{ (GPa)} = AN_a (E_{g \text{ bulk}} + \delta) = AN_a \left[E_{g \text{ bulk}} + \frac{b}{DN_e^{1/3}} \right]. \quad (36)$$

Defining $k = A N_a b/N_e^{1/3}$, Eq. (36) can be simplified to [86],

$$H_{V \text{ nano}} = H_{V \text{ bulk}} + k/D. \quad (37)$$

Eq. (37) indicates that the hardening mechanism of nanocrystalline materials differs from the Hall-Petch relation for coarse-grained materials where $H_{V n} = H_0 + k/D^{1/2}$ [87, 88]. However, Eq. (37) agrees with the result given in [89], showing that the nucleation stress for nanocrystalline materials is inversely proportional to the grain size, $\sigma_n \sim 1/D$.

Hardness and mulliken overlap population

Since the first-principles calculation is the current standard model for designing materials, it is highly desirable to estimate the hardness directly from the information of the first-principles calculation. Segall et al. [90, 91] found correlations of overlap population with bond strength. If we take the average overlap population per unit volume of bond to characterize the strength of bond, the relation between hardness and overlap population of crystals is expressed as follow [92]:

$$H_V = AN_a(P/v_b), \quad (38)$$

where N_a is the covalent bond number per unit area, A is a proportional coefficient, P is the Mulliken overlap population [93] and v_b is the bond volume. For crystals with the diamond structure there are 16 bonds in a cell of the cell volume V , the bond volume can then be expressed as $v_b = V/16$. N_a can be expressed as $(16/V)^{2/3}$ or $v_b^{-2/3}$. Thus, their hardness should have the following form [92]:

$$H_V \text{ (GPa)} = APv_b^{-5/3}. \quad (39)$$

For the hardness calculation of crystals with partial metallic bonding like NbN and ReC, a correction of the formula should be considered. The DOS of ReC is shown in Fig. 11, where the vertical line is the Fermi level (E_F) [94]. This phase showed metallic behavior because of finite $N(E_F)$ at the Fermi level. There is a deep valley (E_p) at the left of the Fermi level (E_F), which is named pseudogap. So, the electrons occupying the levels above E_p become delocalized, and the material is said to have metallicity. The number of free electron in a cell can be estimated as [94]

$$n_{\text{free}} = \int_{E_p}^{E_F} N(E) dE, \quad (40)$$

where $N(E)$ is the density of state. The hardness is suggested as

$$H_V \text{ (GPa)} = 740 (P - P')v_b^{-5/3}, \quad (41)$$

where, P' is metallic Mulliken population and

$$P' = n_{\text{free}}/V. \quad (42)$$

Also the metallicity of crystals may be defined as

$$f_m = P' / P. \quad (43)$$

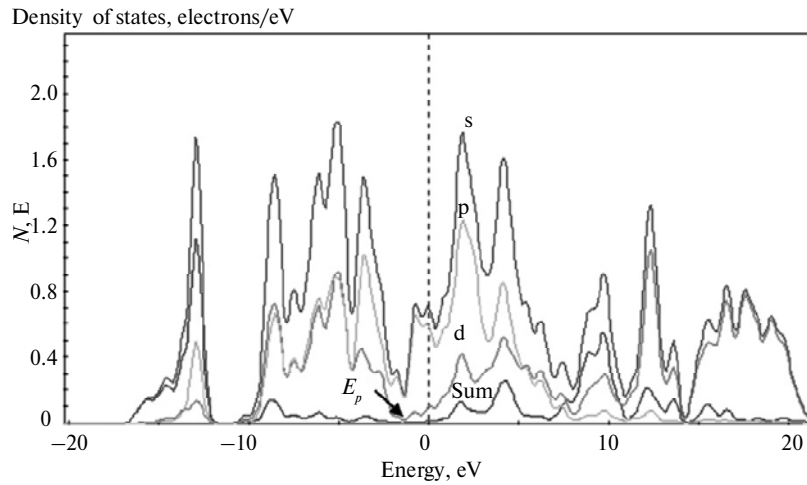


Fig. 11. DOS of ReC. $N(E)$ is the density of state, E_p is the pseudogap energy.

It is to be noted that owing to the high sensitivity of Mulliken population to the basis set [95], constant A in Eq. (38) depends also on the basis set. The typical value of A in Eq. (38) is 740. Figure 12 shows the relationship between the hardness calculated by Mulliken population and the experimental values of hardness. From the inset in Fig. 12, it can be seen that although a few data appear relative big error, the variation trend of Mulliken population hardness and experimental hardness is accordant. Especially for individual classes of materials, Mulliken population hardness method may provide good predictions. The calculated hardness values of crystals with partial metallic bonding are listed in Table 4. The results show that ReC has high hardness of 29.4 GPa, which agrees with its measurement value [35]. Contrarily, IrC exhibits low hardness value due to high metallicity.

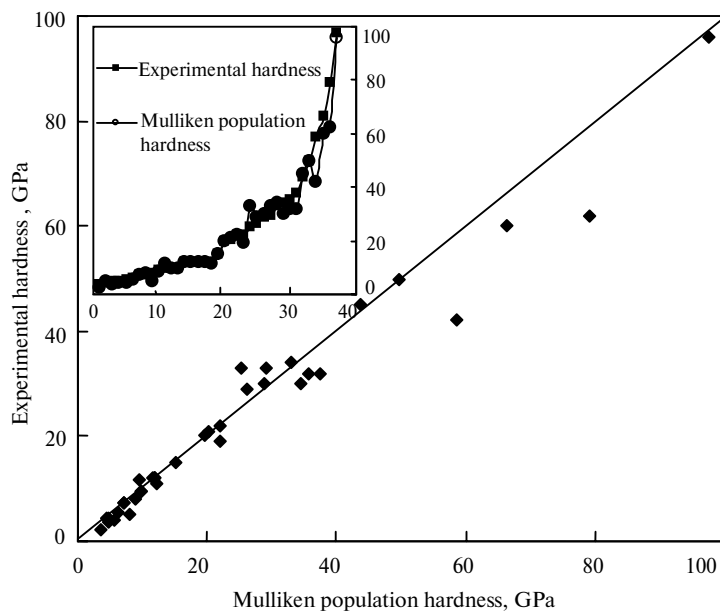


Fig. 12. Comparison between the hardness calculated by Mulliken population and the experimental values of hardness.

Table 4. Mulliken population hardness of transition metal compounds [94]. The bond length, d (Å), Mulliken bond overlap population, P , the volume of bond, v_b (Å³), calculated hardness, $H_{V\text{calc}}$ (GPa), and available experimental Vickers hardness, $H_{V\text{exp}}$ (GPa)

	Structure	D , Å	P	P'	f_m	v_b , Å ³	$H_{V\text{calc}}$	$H_{V\text{exp}}$
HfC	NaCl	2.344	0.408	0.008	0.02	4.293	26.1	25.5
TaC	NaCl	2.213	0.41	0.066	0.16	3.613	30.1	29.0
WC	WC	2.223	0.38	0.019	0.05	3.590	31.8	30 ± 3
ReC	WC	2.157	0.34	0.054	0.16	3.271	29.4	
OsC	WC	2.165	0.317	0.089	0.28	3.347	22.7	
IrC	WC	2.192	0.317	0.143	0.45	3.501	15.9	
TiC	NaCl	2.159	0.333	0.006	0.02	3.353	32.3	28.6, 29 ± 3
ZrC	NaCl	2.344	0.35	0.007	0.02	4.297	22.5	25.8
TiN	NaCl	2.112	0.278	0.055	0.20	3.167	24	23
ZrN	NaCl	2.288	0.27	0.043	0.16	3.994	16.7	15
HfN	NaCl	2.314	0.325	0.044	0.14	4.131	19.4	15.9, 17 ± 2
VN	NaCl	2.067	0.262	0.128	0.49	2.944	16.3	13, 15 ± 1
NbN	NaCl	2.204	0.247	0.094	0.38	3.567	13.6	13, 14 ± 1

These theoretical hardness approaches have been employed to the hardness calculations for the hard materials [96—106]. These studies indicate that microscopic models of hardness possess a good predictive power especially for strong covalent solids.

Anisotropy of hardness is also a very interesting topic. Recently, Šimůnek has suggested a method to calculate the anisotropy of hardness [107]. We may also employ Eq. (30) to study the anisotropy of hardness in the crystals, when n^μ is taken as the number of bond of type μ along a direction of the crystal. It should be noted that in some cases, a primary slip plane may play a dominant role in anisotropy of hardness.

According to the above microscopic models of hardness, three conditions should be met for a superhard material: higher bond density or electronic density, shorter bond length, and greater degree of covalent bonding. A class of superhard materials is thus expected to be compounds with the shortest bond lengths; these are composed of the light elements from periods 2 and 3 of the periodic table. Recent synthesis of BC₅ [108], B₂₈ [9, 10], and M-carbon [22] indicate that the covalent and polar-covalent compounds formed by light elements still play an important role in search for superhard materials. Another relatively new field of research is borides, carbides and nitrides of dense transition metals, since dense transition metals, such as the 5d metals, have the high valence electron densities. The introduction of light metals into a boron network should also deserve investigation, for example, B₁₃N₂ [80], B₁₂N₂Be [77]. Nanocrystallinity is a means for further hardening of the traditional superhard bulk materials. However, a further study on hardening mechanism in nanoceramics is still necessary. The microscopic hardness models introduced here can play an important role in designing superhard materials.

This work is supported by the National Natural Science Foundation of China (Grant 50672080).

Зроблено огляд останніх розробок в області мікромоделей твердості. У цих моделях теоретичну твердість описано як функцію щільності та міцності зв'язку. Міцність зв'язку може бути охарактеризована шириною забороненої зони, опорним потенціалом, енергією утримання електрона або вільною енергією Гіббса. Тому різні вирази міцності зв'язку приведуть до різних моделей міцності. Зокрема, докладно описано модель твердості, основувану на теорії хімічного зв'язку складних кристалів. Наведено приклади розрахунків твердості типових кристалів, таких як шпінель S_3N_4 , стишовіт SiO_2 , $B_{12}O_2$, ReB_2 , OsB_2 , RuB_2 і PtN_2 . Ці мікромоделі твердості будуть грати важливу роль в пошуку нових твердих матеріалів.

Ключові слова: твердість, модуль об'ємного стиснення, модуль зсуву, іонність, надтверді матеріали.

Дан обзор последних разработок в области микромоделей твердости. В этих моделях теоретическая твердость описана как функция плотности и прочности связи. Прочность связи может быть охарактеризована шириной запрещенной зоны, опорным потенциалом, энергией удержания электрона или свободной энергией Гиббса. Поэтому различные выражения прочности связи приведут к различным моделям твердости. В частности, подробно описана модель твердости, основанная на теории химической связи сложных кристаллов. Привены примеры расчета твердости типичных кристаллов, таких как шпинель S_3N_4 , стишовит SiO_2 , $B_{12}O_2$, ReB_2 , OsB_2 , RuB_2 и PtN_2 . Эти микромоделі твердости будут играть важную роль в поиске новых твердых материалов.

Ключевые слова: твердость, модуль объемного сжатия, модуль сдвига, ионность, сверхтвердые материалы.

1. McColm I. J. Ceramic Hardness. — New York: Plenum Press, 1990.
2. Handbook of Ceramic Hard Materials: V. 1, 2 // Ed. R. Riedel. — Weinheim: WILEY-VCH Verlag, Germany, 2000.
3. Shaw M. C. The fundamental basis of the hardness test. Chapter 1 // The science of hardness testing and its research applications / Ed. J. H. Westbrook and H. Conrad. — Ohio, USA: American Society for Metals, Metals Park, 1973.
4. Szymanski A., Szymanski J. M. Hardness estimation of minerals rocks and ceramic materials. — Amsterdam: Elsevier, 1989.
5. Glazov V. M., Vigdorovich V. N. Mikrotverdoct' metallov (Microhardness of metals). — Moskva: Metallurgiya, 1969.
6. Gilman J. J. Why silicon is hard // Science. — 1993. — **261**, N 5127. — P. 1436—1439.
7. Veprek S. The search for novel superhard materials // Vac. Sci. Technol. A. — 1999. — **17**, N 5. — P. 2401—2420.
8. Levine J. B., Tolbert S. H., Kaner R. B. Advancements in the search for superhard ultra-incompressible metal borides // Adv. Funct. Mater. — 2009. — **19**. — P. 3519—3533.
9. Oganov A. R., Chen J., Gatti C. et al. Ionic high pressure form of elemental boron // Nature. — 2009. — **457**, N 7231. — P. 863—867.
10. Oganov A. R., Solozhenko V. L. Boron: a hunt for superhard polymorphs // J. Superhard Materials. — 2009. — **31**, N 5. — P. 3—11.
11. Solozhenko V. L., Andrault D., Fiquet G. et al. Synthesis of superhard cubic BC_2N // Appl. Phys. Lett. — 2001. — **78**, N 10. — P. 1385—1387.
12. Irifune T., Kurio A., Sakamoto S. et al. Ultrahard polycrystalline diamond from graphite // Nature. — 2003. — **421**, N 6923. — P. 599—600.
13. Wang Z., Zhao Y., Tait K. et al. Quenchable superhard carbon phase synthesized by cold compression of carbon nanotubes // Proc. Nat. Acad. Sci., U.S.A. — 2004. — **101**, N 38. — P. 13699—13702.
14. Dubrovinskaia N., Dubrovinsky L., Crichton W. et al. Aggregated diamond nanorods, the densest and least compressible form of diamond // Appl. Phys. Lett. — 2005. — **87**, N 8. — P. 083106 1—3.
15. Dubrovinsky L. S., Dubrovinskaia N. A., Swamy V. et al. The hardest known oxide // Nature. — 2001. — **410**, N 6829. — P. 653—654.
16. Brazhkin V., Dubrovinskaia N., Nicol M. et al. What does “Harder than Diamond” mean? // Nature Materials. — 2004. — **3**, N 2. — P. 576—577.

17. *Dubrovinskaja N., Solozhenko V. L., Miyajima N. et al.* Superhard nanocomposite of dense polymorphs of boron nitride: Noncarbon material has reached diamond hardness // *Appl. Phys. Lett.* — 2007. — **90**, N 10. — P. 101912 1—3.
18. *Liu A.Y., Cohen M. L.* Prediction of new low compressibility solids // *Science.* — 1989. — **245**, N 4920. — P. 841—842.
19. *Teter D. M., Hemley R. J.* Low compressibility carbon nitrides // *Ibid.* — 1996. — **271**, N 5245. — P. 53—55.
20. *Kroll P.* Hafnium Nitride with thorium phosphide structure: physical properties and an assessment of the Hf—N, Zr—N, and Ti—N phase diagrams at high pressures and temperatures // *Phys. Rev. Lett.* — 2003. — **90**, N 12. — P. 125501 1—4.
21. *Shiyou Chen, X. G. Gong, Su-Huai Wei.* Superhard pseudocubic BC₂N superlattices // *Ibid.* — 2007. — **98**, N 1. — P. 015502 1—4.
22. *Q. Li, Ya. Ma, Oganov A. R. et al.* Superhard monoclinic polymorph of carbon // *Ibid.* — 2009. — **102**, N 17. — P. 175506 1—4.
23. *Wang H., Li Q., Li Y. et al.* Ultra-incompressible phases of tungsten dinitride predicted from first principles // *Phys. Rev. B.* — 2009. — **79**, N 13. — P. 132109 1—6.
24. *Li Q., Wang M., Oganov A. R. et al.* Rhombohedral superhard structure of BC₂N // *J. Appl. Phys.* — **105**, N 5. — P. 053514 1—4.
25. *Zhang M., Wang M., Cui T. et al.* Electronic structure, phase stability, and hardness of the osmium borides, carbides, nitrides, and oxides: First-principles calculations // *J. Phys. Chem. Solids.* — 2008. — **69**, N 8. — P. 2096—2102.
26. *Li Y., Wang H., Li Q. et al.* Twofold coordinated ground-state and eightfold high-pressure phases of heavy transition metal nitrides MN₂ (M = Os, Ir, Ru and Rh) // *Inorganic Chemistry.* — 2009. — In press.
27. *Haines J., Leger J. M., Bocquillon G.* Synthesis and design of superhard materials // *Annu. Rev. Mater. Res.* — 2001. — **31**. — P. 1—23.
28. *Hong S., Jhi S. H., Roundy D. et al.* Structural forms of cubic BC₂N // *Phys. Rev. B.* — 2001. — **64**, N 9. — P. 094108.
29. *He J. L., Guo L. C., Wu E. et al.* First-principles study of B₂CN crystals deduced from the diamond structure // *J. Physics-Condensed Matter.* — 2004. — **16**, N 46. — P. 8131—8138.
30. *Wang Y. X., Masao A., Taizo S., Fan Z.* Ab initio study of monoclinic iridium nitride as a high bulk modulus compound // *Phys. Rev. B.* — 2007. — **75**, N 10. — P. 104110 1—6.
31. *Gilman J. J.* Electronic basis of hardness and phase transformations // *J. Phys. D: Appl. Phys.* — 2008. — **41**, N 7. — P. 074020—074024.
32. *Cohen M. L.* Calculation of bulk moduli of diamond and zinc-blende solids // *Phys. Rev. B.* — 1985. — **32**, N 12. — P. 7988—7991.
33. *Zhang S., Li H., Li H. et al.* Calculation of the bulk modulus of simple and complex crystals with the chemical bond method // *J. Phys. Chem. B.* — 2007. — **111**, N 6. — P. 1304—1309.
34. *Sung C. M., Song M.* Carbon nitride and other speculative superhard materials // *Mater. Chem. Phys.* — 1996. — **43**, N 1. — P. 1—18.
35. *Brazhkin V., Lyapin A., Hemley R. J.* Harder than diamond: dreams and reality // *Philosophical Magazine A.* — 2002. — **82**, N 2. — P. 231—253.
36. *Ceder G.* Predicting Properties from Scratch // *Science.* — 1998. — **280**, N 5366. — P. 1099—1100.
37. *Teter D. M.* Computational alchemy: The search for new superhard materials // *Mater. Res. Soc. Bull.* — 1998. — **23**, N 1. — P. 22—27.
38. *Gilman J. J.* Hardness — a strength microprobe. Chapter 4 // *The science of hardness testing and its research applications* / Eds. by J. H. Westbrook, H. Conrad. — Ohio, USA: American Society for Metals, Metals Park, 1973.
39. *Nye J. F.* Physical properties of crystals. — London: Oxford University Press, 1957.
40. *Hill A.* The elastic behaviour of a crystalline aggregate // *Proc Phys. Soc.* — 1952. — **65**. — P. 349—354.
41. *Gao F. M., He J. L., Wu E. D. et al.* Hardness of covalent crystals // *Phys. Rev. Lett.* — 2003. — **91**, N 1. — P. 015502 1—4.
42. *Gao F. M.* Hardness estimation of complex oxide materials // *Phys. Rev. B.* — 2004. — **69**, N 9. — P. 094113 1—6.
43. *Simunek A., Vackar J.* Hardness of covalent and ionic crystals: First-principle calculations // *Phys. Rev. Lett.* — 2006. — **96**, N 8. — P. 085501 1—4.
44. *Simunek A.* How to estimate hardness of crystals on a pocket calculator // *Phys. Rev. B.* — 2007. — **75**, N 17. — P. 172108 1—4.

45. Li K., Wang X., Zhang K., Xue D. Electronegativity identification of novel superhard materials // *Phys. Rev. Lett.* — 2008. — **100**, N 23. — P. 235504 1—4.
46. Li K., Xue D. Hardness of materials: Studies at levels from atoms to crystals // *Chinese Science Bulletin.* — 2009. — **54**, N 1. — P. 131—136.
47. Mukhanov V. A., Kurakevych O. O., Solozhenko V. L. The Interrelation between the *hardness* and compressibility of substances and their structure and their structure and thermodynamic properties // *J. Superhard Materials.* — 2008. — **30**, N 6. — P. 10—22.
48. Pauling L. The nature of the chemical bond. — Ithaca, New York: Cornell Univ. Press, 1960. — 91 p.
49. Shanker J., Verma M. P. The fractional ionic character of alkali and silver halide crystals // *Pramana.* — 1973. — **1**, N 6. — P. 243—246.
50. Hidaka T. Pauling's ionicity and Phillips' ionicity // *J. Phys. Soc. Japan.* — 1978. — **44**, N 4. — P. 1204—1207.
51. Phillips J. C. Ionicity of the chemical bond in crystals // *Rev. Mod. Phys.* — 1970. — **42**, N 3. — P. 317—356.
52. Van Vechten J. A. Quantum dielectric theory of electronegativity in covalent systems // *Phys. Rev. B.* — 1969. — **182**, N 3. — P. 891—905.
53. Van Vechten J. A. Quantum dielectric theory of electronegativity in covalent systems. II. Ionization potentials and interband transition energies // *Ibid.* — 1969. — **187**, N 3. — P. 1007—1020.
54. Levine B. F. Bond susceptibilities and ionicities in complex crystal structures // *J. Chem. Phys.* — 1973. — **59**, N 3. — P. 1463—1485.
55. Levine B. F. Bond-charge calculation of nonlinear optical susceptibilities for various crystal structures // *Phys. Rev. B.* — **7**, N 6. — P. 2600—2626.
56. Zhang S. Y. Investigation of chemical bonds on complex crystals // *Chin. J. Chem. Phys.* — 1991. — **4**. — P. 109—115.
57. Zhang S. Y., Gao F. M., Wu C. X. Chemical bond properties of rare earth ions in crystals // *J. Alloys Compd.* — 1998. — **275—277**. — P. 835—837.
58. Gao F. M., Zhang S. Y. Investigation of covalency and spectrum shifts in *3d* transition-metal compounds // *Chin. J. Inorg. Chem.* — 2000. — **16**, N 5. — P. 751—756.
59. Gao F. M., Li D. C., Zhang S. Y. Mossbauer spectroscopy and chemical bonds in BaFe₁₂O₁₉ hexaferrite // *J. Phys.-Cond. Matter.* — 2003. — **15**, N 29. — P. 5079—5084.
60. Krell A. Vickers hardness and microfracture of single and polycrystalline Al₂O₃ // *Kristall und Technik.* — 1980. — **15**, N 12. — S. 1467—1474.
61. Luo S. N., Swadener J. G., Ma C., Tschauer O. Examining crystallographic orientation dependence of hardness of silica stishovite // *Physica B.* — 2007. — **399**, N 6. — P. 138—142.
62. Brazhkin V. V., Grimsditch M., Guedes I. et al. Elastic moduli and the mechanical properties of stishovite single crystals // *Phys. Uspekhi.* — 2002. — **45**, N 4. — P. 447—448.
63. Zerr A., Miehe G., Serghiou G. et al. Synthesis of cubic silicon nitride // *Nature.* — 1999. — **400**, N 6742. — P. 340—342.
64. Mo S. D., Ouyang L., Ching W. Y. et al. Interesting Physical properties of the new spinel phase of Si₃N₄ and C₃N₄ // *Phys. Rev. Lett.* — 1999. — **83**, N 24. — P. 5046—5049.
65. Sekine T., Mitsuhashi T. High-temperature metastability of cubic spinel Si₃N₄ // *Appl. Phys. Lett.* — 2001. — **79**, N 17. — P. 2719 1—3.
66. Gao F. M., Xu R., Liu K. Origin of hardness in nitride spinel materials // *Phys. Rev. B.* — 2005. — **71**, N 5. — P. 052103 1—4.
67. Soignard E., Somayazulu M., Dong J. et al. High pressure-high temperature synthesis and elasticity of the cubic nitride spinel γ -Si₃N₄ // *J. Phys. C.* — 2001. — **13**(22). — P. 557—563.
68. Jiang J. Z., Kragh F., Frost D. J. et al. Hardness and thermal stability of cubic silicon nitride // *J. Phys.: Condens. Matter.* — 2001. — **13**, N 22. — P. L515—L520.
69. Zerr A., Kempf M., Schwarz M. et al. Elastic moduli and hardness of cubic silicon nitride // *J. Am. Ceram. Soc.* — 2002. — **85**, N 1. — P. 86—90.
70. Chung H. Y., Weinberger M. B., Levine J. B. et al. Synthesis of ultra-incompressible superhard rhenium diboride at ambient pressure // *Science.* — 2007. — **316**, N 5823. — P. 436—439.
71. Qin J., He D., Wang J. et al. Is rhenium diboride a superhard material? // *Adv. Mater.* — 2008. — **20**, N 24. — P. 4780—4783.

72. Cumberland R. W., Weinberger M. B., Gilman J. J. et al. Osmium diboride, an ultra-incompressible, hard material // J. Amer. Chem. Soc. — 2005. — **127**, N 20. — P. 7264—7265.
73. Crowhurst J.C., Goncharov A. F., Sadigh B. et al. Synthesis and characterization of the nitrides of platinum and iridium // Science. — 2006. — **311**, N 5765. — P. 1275—1278.
74. Gu Q., Krauss G., Steurer W. Transition metal borides: superhard versus ultra-incompressible // Adv. Mater. — 2008. — **20**. — P. 3620—3626.
75. Emin D., Aselage T. L., Switendick A. C. et al. Boron-rich solids. — New York: AIP, 1990.
76. Hubert H., Devouard B., Garvie L. A. J. et al. Icosahedral packing of B₁₂ icosahedra in boron suboxide (B₆O). // Nature. — 1998. — **391**. — P. 376—378.
77. Gao F. M., Hou L., He Y. H. Origin of superhardness in icosahedral B-12 materials // J. Phys. Chem. B. — 2004. — **108**, N 35. — P. 13069—13073.
78. Gao F. M., Qin X. J., Wang L. Q. et al. Prediction of new superhard boron-rich compounds // J. Phys. Chem. B. — 2005. — **109**, N 31. — P. 14892—14895.
79. Olofsson M., Lundstrom T. Synthesis and structure of non-stoichiometric B₆O // J. Alloys. Compounds. — 1997. — **257**, N 1—2. — P. 91—95.
80. Kurakevych O. O., Solozhenko V. L. Rhombohedral boron subnitride, B₁₃N₂, by X-ray powder diffraction // Acta Crystallogr. Sect. C. — 2007. — **63**. — P. i80—i82.
81. Solozhenko V. L., Kurakevych O. O., Oganov A. R. On the hardness of a new boron phase, orthorhombic γ -B28 // J. Superhard Materials. — 2008. — **30**, N 6. — P. 428—429.
82. Gou H. Y., Zhang J. W., Gao F. M. First-principles calculations of boron-rich compounds of B₁₃N₂ and B₁₂C₂X (X = Si, Ge) // J. Phys.-Cond. Matter. — 2008. — **20**, N 50. — P. 505211—505216.
83. Rama Krishna M. V., Friesner R. A. Quantum confinement effects in semiconductor clusters // J. Chem. Phys. — 1991. — **95**, N 11. — P. 8309—8322.
84. Halperin W. P. Quantum size effects in metal particles // Rev. Mod. Phys. — 1986. — **58**, N 3. — P. 533—606.
85. Tse J. S., Klug D. D., Gao F. M. Hardness of nanocrystalline diamonds // Phys. Rev. B. — 2006. — **73**, N 14. — P. 140102 1—4.
86. Gao F. M., Klug D. D., Tse J. S. Theoretical study of new superhard materials: B₄C₃ // J. Appl. Phys. — 2007. — **102**, N 8. — P. 084311 1—5.
87. Andrievski R. A. Superhard materials based on nanostructured high-melting point compounds: achievements and perspectives // Int. J. Refract. Met. Hard Mater. — 2001. — **19**, N 4—6. — P. 447—452.
88. Siegel R. W., Fougere G. E. Mechanical properties of nanophase metals // Nanostruct. Mater. — 1995. — **6**, N 1—4. — P. 205—216.
89. Yamakov V., Wolf D., Phillpot S. R. et al. Deformation-mechanism map for nanocrystalline metals by molecular-dynamics simulation // Nat. Mater. 2004. — **3**, N 1. — P. 43—47
90. Segall M. D., Shah R., Pickard C. J., Payne M. C. Population analysis of plane-wave electronic structure calculations of bulk materials // Phys. Rev. B. — 1996. — **54**, N 23. — P. 16317—16320.
91. Ching W. Y., Xu Y. N. Nonscalability and nontransferability in the electronic properties of the Y—Al—O system // Ibid. — 1999. — **59**, N 20. — P. 12815—12821.
92. Gao F. M. Theoretical model of intrinsic hardness // Ibid. — 2006. — **73**, N 13. — P. 132104 1—4.
93. Mulliken R. S. Electronic Population Analysis on LCAO-MO Molecular Wave Functions. I // J. Chem. Phys. — 1955. — **23**, N 10. — P. 1833—1840.
94. Gou H. Y., Hou L., Zhang J. W., Gao F. M. Pressure-induced incompressibility of ReC and effect of metallic bonding on its hardness // Appl. Phys. Lett. — 2008. — **92**, N 24. — P. 2419011—3.
95. Zhang X., Luo X., Han J. et al. Electronic structure, elasticity and hardness of diborides of zirconium and hafnium: First principles calculations // Computational Mater. Sci. — 2008. — **44**. — P. 411—421.
96. Gou H. Y., Hou L., Zhang J. W. et al. Theoretical hardness of PtN₂ with pyrite structure // Appl. Phys. Lett. — 2006. — **89**, N 14. — P. 141910 1—3.
97. Gou H. Y., Hou L., Zhang J. W. et al. Cubic γ -Be₃N₂: A superhard semiconductor predicted from first principles // Ibid. — 2007. — **90**, N 19. — P. 191905 1—3.
98. Wang Z. B., Gao F. M., Li N. et al. Density functional theory study of hexagonal carbon phases // J. Phys.-Cond. Matter. — 2009. — **21**, N 23. — P. 235401—235406.

99. *Li C. L., Kuo J. L., Wang B. A. et al.* A new layer compound Nb₄SiC₃ predicted from first-principles theory // *J. Phys. D-App. Phys.* — 2009. — **42**, N 7. — P. 075404—075409.
100. *Liu H., Zhu J., Liu Y., Lai Z.* First-principles study on the mechanical properties of vanadium arbedes VC and V₄C₃ // *Mater. Lett.* — 2008. — **62**, N 17—18. — P. 3084—3086.
101. *Chen Z., Gu M., Sun C. Q. et al.* Ultrastiff carbides uncovered in first principles, *Appl. Phys. Lett.* — 2007. — **91**, N 6. — P. 061905 1—3.
102. *Wang M., Li Y., Cui T. et al.* Origin of Hardness in WB₄ and its implications for ReB₄, TaB₄, MoB₄, TcB₄ and OsB₄ // *Ibid.* — 2008. — **93**, N 10. — P. 101905 1—3.
103. *Ribeiro F. J., Tangney P., Louie S. G., Cohen M. L.* Hypothetical Hard Structures of Carbon with Cubic Symmetry // *Phys. Rev. B.* — 2006. — **74**, N 17. — P. 172101 1—4.
104. *Smedskjaer M. M., Jensen M., Yue Y. Z.* Theoretical calculation and measurement of the hardness of diopside // *J. Amer. Ceram. Soc.* — 2008. — **91**, N 2. — P. 514—518.
105. *Gao L. H., Gao F. M.* Chemical bond properties and hardness estimation of rare earth garnets // *Mater. Chem. Phys.* — 2009. — **113**, N 1. — P.145—149.
106. *Gou H. Y., Hou L., Zhang J. W. et al.* First-principles study of low compressibility osmium borides // *Appl. Phys. Lett.* — 2006. — **88**, N 22. — P. 221904 1—3.
107. *Šimůnek A.* Anisotropy of hardness from first principles: The cases of ReB₂ and OsB₂ // *Phys. Rev. B.* — 2009. — **80**, N 6. — P. 060103 1—4.
108. *Solozhenko V. L., Kurakevych O., Andraut D. et al.* Ultimate metastable solubility of boron in diamond: synthesis of superhard diamondlike BC₅ // *Phys. Rev. Lett.* — 2009. — **102**. — P. 015506 1—4.

Key Laboratory of Applied Chemistry,
Yanshan University

Received 25.11.09